

Analyzing the impact of vibrations on E-ELT primary segmented mirror

B. Sedghi^a, M. Müller^a, and M. Dimmler^a

^aEuropean Southern Observatory (ESO), Karl-Schwarzschild-Strasse 2, Garching, Germany

ABSTRACT

The E-ELT primary mirror is 39m in diameter composed of 798 segments. It is exposed to external large but slow amplitude perturbations, mostly gravity, thermal and wind. These perturbations are efficiently rejected by a combination of edge sensor loop and adaptive optics (AO) in order to leave a small residual wavefront error (WFE). Vibrations induced by various equipment in the observatory are typically smaller amplitude but higher frequency perturbations exceeding the rejection capabilities of these control loops. They generate both, low spatial frequency and high spatial frequency WFE. Especially segment phasing errors, i.e. high spatial frequency errors, cannot be compensated by AO. The effect of vibrations is characterized by excitation sources and transmission of the telescope structure and segment support. They all together define the WFE caused by M1 due to vibrations. It is important to build a proper vibration error budget and specification requirements from an early stage of the project. This paper presents the vibration analysis and budgeting approach developed for E-ELT M1 and addresses the impact of vibrations onto WFE.

Keywords: E-ELT, primary segmented mirror, modeling, control, dynamical simulation, vibration, error budget, wavefront error

1. INTRODUCTION

The European Extremely Large Telescope (E-ELT) is a project led by ESO for a next generation optical and near-infrared, ground-based telescope. Its optical design is based on a three-mirror anastigmat with two folding flat mirrors sending the beam to either of the two Nasmyth foci along the elevation axis of the telescope. The elliptical primary mirror consists of 798 off-axis aspherical segments, each 1.4 m in size and 50 mm thick. The secondary and tertiary mirrors are designed as convex and concave aspherical mirrors, respectively, providing active position and shape control. The quarternary mirror is adaptive aiming at the compensation of fast wavefront distortions which are mainly due to atmospheric turbulence. The main purpose of the ultra-lightweight fifth mirror is to provide the compensation of image motion. The mirror units (M1– M5) are held by the main structure, which also supports the instruments at the Nasmyth platforms, all handling tools and all equipment necessary for the altitude azimuth kinematics. The main structure also holds the pre-focal stations, which contain the on-sky metrology for wavefront control.

To analyze the impact of various error sources such as gravity, temperature, wind, vibration and turbulence, different models and simulation environments and tools were developed to account for the different temporal and spatial frequencies of perturbations.¹ The objective of the modeling tools is not only to predict the performance of the telescope but also to derive requirements for subsystems, to 'understand' the behavior of the subunits in the telescope, and to quantify the impact of various control strategies. The tools are extensively used to provide feedback to the project and the system engineering team, and to generate error budgets.

One of the main contributors to wavefront error are excitations induced by different equipment in the observatory. The forces generated by these devices are exciting the mechanical resonant modes of the telescope structure and hosted units. These excitation sources (not necessarily having a periodic nature), their transmission through the mechanical structure and their impact on the performance are called 'vibrations'.

Further author information: (Send correspondence to B. Sedghi)
B. Sedghi: E-mail: bsedghi@eso.org, Telephone: +49 89 32006529

The vibration excitations generate both, low spatial frequency and high spatial frequency WFE. The low spatial error predominates the image jitter and involves motions of all mirrors, whereas the primary segmented mirror is a potential source for generating high spatial frequency WFE, which cannot be efficiently compensated by AO loops. Due to its sensitivity to vibrations, involvement of different trade-offs, e.g. choice of segment position actuators, and modeling and analysis complexity, dedicated vibration analysis and error budgeting are preformed for E-ELT segmented M1. The general concept of the approach follows the main lines presented in detail in,² where a model based sensitivity analysis is used as a basis for estimating and defining the engineering budgets. A similar approach is also undertaken by the TMT project.^{3,4}

In this paper, the analysis and budgeting approach for the M1 segmented mirror is presented. Section 3 introduces the modeling assumptions and analysis tools. In Section 4 the analysis results through some examples are illustrated. The requirement and vibration budgeting approach with an example is presented in Section 5. Finally, Section 6 concludes the paper.

2. E-ELT MODELING AND VIBRATION SENSITIVITY ANALYSIS: OVERVIEW

Using the finite element model (FEM) of the telescope structure and mirror units, the optical sensitivity and the knowledge of the wavefront control correction capability, the transmission of vibration from sources to the wavefront error can be estimated. Consequently, one can estimate the acceptable amplitude of vibrational sources that satisfy the top-level performance budget.

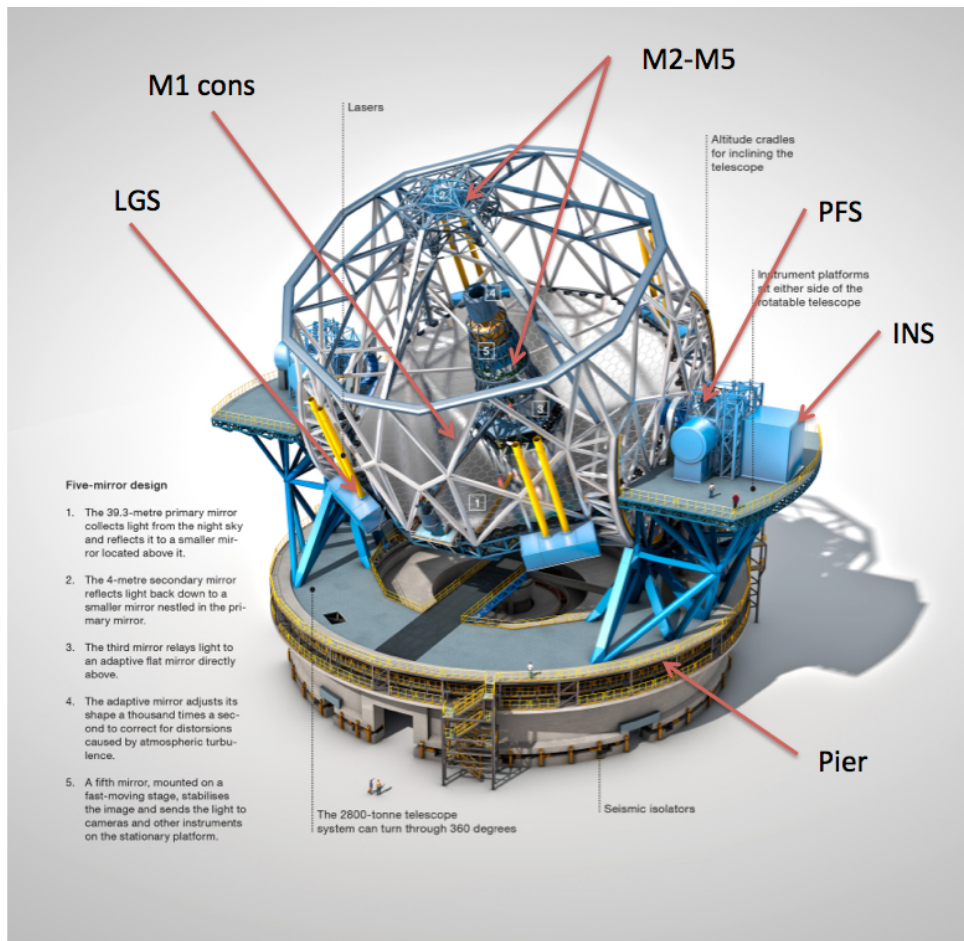


Figure 1. A view of E-ELT, primary segmented mirror and location of main vibration sources

The key element of the engineering budget derivation is the sensitivity analysis to determine the transmission responses of the various potential vibrational sources in the observatory onto the telescope to the wavefront. In the FEM of the telescope (see Figure 1) several locations are assumed as the input points at which the telescope can be potentially excited by vibration sources. These locations are mainly distributed and categorized based on the telescope product tree for which separate engineering vibrational requirements need to be derived. Each contributor includes different sources of vibration. For instance, cooling lines and cable wraps are the sources of vibration belonging to the Main Structure, while pumps, chillers and air handlers belong to dome and facility buildings. The input sources of vibration in the FEM are as follows:

- Dome and Main Structure: mainly input from telescope pier
- Instruments (INS): six instruments located at the Nasmyth platforms
- Prefocal stations (PFS): two input sources, one on each Nasmyth platform
- Laser Guide Stars (LGS): four laser units at the location of the launching telescopes
- M2 to M5 units: a separate input source at the center of gravity of each unit
- M1 unit: More than hundred electronic concentrator (M1 cons.) cabinets uniformly distributed over the M1 cell structure

In addition, the model has inputs for each actuator of the primary segments for designing and including the position actuator servo loops. For trade-off purposes two variations of the model are available, each model represented by one type of actuator, i.e. i) hard actuators (piezo based, with high mechanical stiffness), ii) soft actuators (voice-coil based with low mechanical stiffness).

The model has several outputs including the six degree of freedom (6DOF) motions of each mirror unit, each of the 798 segments, and interface motions of telescope structure to the hosted units e.g. interface points of hexapods of the M2 and M3 units to the telescope main structure in (x, y, z) directions and interface between the telescope and the instruments. In addition, the model provides outputs representing the sensor readings of each M1 segment actuator. These outputs with combination of the inputs to the actuators are used to characterize the segment actuator internal servo-loops. By combining the closed-loop actuator servo-loop to the mechanical model the important dynamical effects such as the electronic stiffness (required for the soft actuators), or the active damping (in case of hard actuators),⁵ are realistically represented.

The FEM model of the telescope structure has 15000 modes (30000 states) including detailed model of M1, M2 and M3 units. The M1 unit model includes the segment subunit dynamics for all 798 segments (representing the segment support system and actuator stiffness). The common practice is to transform the FE models to state-space models represented by $[A, B, C, D]$ matrices. The models are initially developed in Matlab using the functionalities of the Matlab Control System Toolbox. The main difficulty and complexity of M1 segmented system analysis and simulation using these traditional tools comes from two fundamental properties of the system: i) the dynamics 'of each segment' up to the interested vibrational frequencies shall be preserved, therefore the model order reduction technics are not efficient, i.e a valid model still has a high order, ii) high number of inputs, 2394 (798×3) for segment actuator commands, and outputs, 4788 ($798 \times 3 \times 2$) signals representing the piston/tip/tilt (PTT) motion of each segment and the encoder reading of each actuator, require large computing power and memory.

To solve this issue, the FE models are transformed to Matlab data objects using the Structural Modeling Toolbox (SMI).⁶ The toolbox takes advantage of the fixed structure and the sparsity of the matrices $[A, B, C, D]$ building a 'modal' state-space model. The modal state-space objects store only the data required. Additionally input- and output-names, input- and output-groups as well as a structure with information about the source data files and the model history are stored. With the object modal state-space models analog commands to those of Matlab Control System Toolbox are available, e.g. `bode` or `freqresp` to compute the frequency response matrix $\mathbf{G}(\omega)$ with magnitude and phase directly based on the modal expression of the transfer function matrix (between input u_j and output y_i). The SMI-Toolbox provides the frequency responses much faster and more efficient.

3. M1 MODELING AND VIBRATION SENSITIVITY ANALYSIS: APPROACH

Figure 2 shows the PACT servo-loop closed-loop scheme of vibration transmission responses to the piston,tip and tilt of the primary mirror segments.

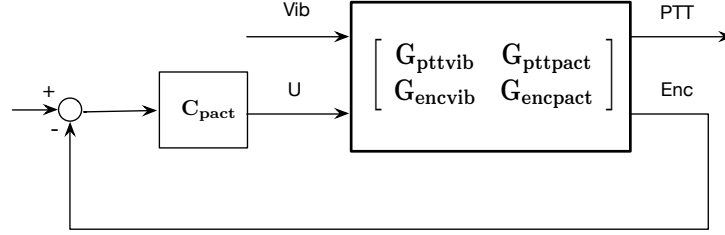


Figure 2. Vibration to segment PTT block diagram scheme including the actuator servo-loop feedback control

The approach for deriving the vibration sensitivity responses for the M1 mirror is as follows: The frequency responses from each vibration source input to the PTT of each segment in closed loop (position actuator internal servo-loop) are calculated. This is performed for each frequency ω in the frequency interval of interest and using the following matrix manipulations:

$$\mathbf{H}_{\text{pttvib}}(j\omega) = \mathbf{G}_{\text{pttvib}}(j\omega) - \mathbf{G}_{\text{pttpact}}(j\omega)[\mathbf{I}_{n \times n} + \mathbf{C}_{\text{pact}}(j\omega)\mathbf{G}_{\text{encpact}}(j\omega)]^{-1}\mathbf{C}_{\text{pact}}(j\omega)\mathbf{G}_{\text{encvib}}(j\omega) \quad (1)$$

where $\mathbf{H}_{\text{pttvib}}(j\omega)$ is the frequency response matrix from vibration inputs to the PTT motions of all segments with closed-loop actuators, $\mathbf{G}_{\text{pttvib}}(j\omega)$, $\mathbf{G}_{\text{pttpact}}(j\omega)$ are the open-loop frequency response matrices from vibration inputs and actuator commands to the PTT motions of each segment, respectively. $\mathbf{G}_{\text{encvib}}(j\omega)$, $\mathbf{G}_{\text{encpact}}(j\omega)$ are the open-loop frequency response matrices from vibration inputs and actuator commands to the actuator encoder readings, respectively.

$$\mathbf{C}_{\text{pact}}(j\omega) = \text{diag}\{C_{\text{pact}}(j\omega)\} = C_{\text{pact}}(j\omega)\mathbf{I}_{n \times n} \quad (2)$$

is the actuator servo loop controller matrix where $\mathbf{I}_{n \times n}$ is an identity matrix with $n = 2394$, and C_{pact} represents the single-input single-output (SISO) controller implemented for each PACT.

Although the toolbox provides a fast and efficient frequency response calculation from the FEM model, however due to the large size of matrices and particularly closed-loop calculation involving inverting large matrices (see Eq. 1), the frequency response calculations require large computing power and computer memory. Once these responses are calculated and stored they can be used efficiently for post processing, i.e. wavefront calculation, transformation of PTT motions to spatial mirror modes, e.g. actuator-edge sensor interaction matrix ($IM = PACT2ES$) SVD modes. The frequency response analysis is used to derive the sensitivity responses of different vibration sources to the wavefront error. The analysis is complemented with time domain simulations to crosscheck and verify the frequency responses and also to derive the final performance.

The time response of the segment motions for a given vibration input (force or acceleration) $u_{\text{vib}}(t)$ can be calculated by an inverse Fourier transformation `ifft`, i.e.

$$PTT(t) = \mathcal{F}^{-1}(\mathbf{H}_{\text{pttvib}}(j\omega)\mathbf{U}_{\text{vib}}(j\omega)) \quad (3)$$

where $\mathbf{U}_{\text{vib}}(j\omega)$ is the vector of the Fourier transform of vibration input signals $u_{\text{vib}}(t)$. To verify and cross-check the validity of the results, the time series were compared against those derived from specific test cases by reducing the order of the model and performing direct time domain simulations (ODE solvers). In the next section examples of vibration sensitivity and performance analysis are presented.

4. M1 VIBRATION SENSITIVITY ANALYSIS AND PERFORMANCE ESTIMATION: EXAMPLES

For different vibration sources assumed for the telescope (see the list in Section 3) the sensitivity responses $\mathbf{H}_{\text{pttvib}}(j\omega)$ (Eq. 1) are derived. Different case studies assuming different type of actuators, servo-loop control and damping strategies are also taken into account. The comparison and results for different case studies are not specifically discussed here and are out of the scope of this paper. Here, the analysis tools and typical responses and behavior of the M1 segments due to the potential vibration sources are shown.

There are different ways and metrics to express the performance of the M1 mirror to vibrations. The vibration response expressed as PTT of each segment alone is not a good metric or criterion for understanding the behavior of the system. The common metric and criterion is the wavefront error expressed as:

$$WFE_{M1} = \sqrt{\frac{\sum_{i=1}^{798} PTT^2 op_i}{798}} = \frac{\|PTT op\|_2}{\sqrt{798}} \quad (4)$$

where $\|PTT op\|_2$ is the norm-2 of the vector of all segment optical PTTs, $Pop_i = 2 * P_i$, $TT op_i = 0.64 * TT_i$ are the scaling factors converting the mechanical PTTs to the optical PTTs. Two different matrix norms are good candidates to relate the M1 wavefront WFE_{M1} to the various vibration input sources: norm-2 and Frobenius norms of $\mathbf{H}_{\text{pttvib}}(j\omega)$ for each frequency ω , i.e. $\|\mathbf{H}_{\text{pttvib}}(j\omega)\|_2 = \bar{\sigma}(\mathbf{H}_{\text{pttvib}}(j\omega))$ where $\bar{\sigma}$ is the maximum singular value of the matrix, and $\|\mathbf{H}_{\text{pttvib}}(j\omega)\|_F = \sqrt{\sum_{i,k} |H_{\text{pttvib},i,k}(j\omega)|^2}$.

From the definition of the Frobenius norm it can be observed that it provides directly the WFE rms if uncorrelated normalized vibration sources are assumed to be acting on the system.

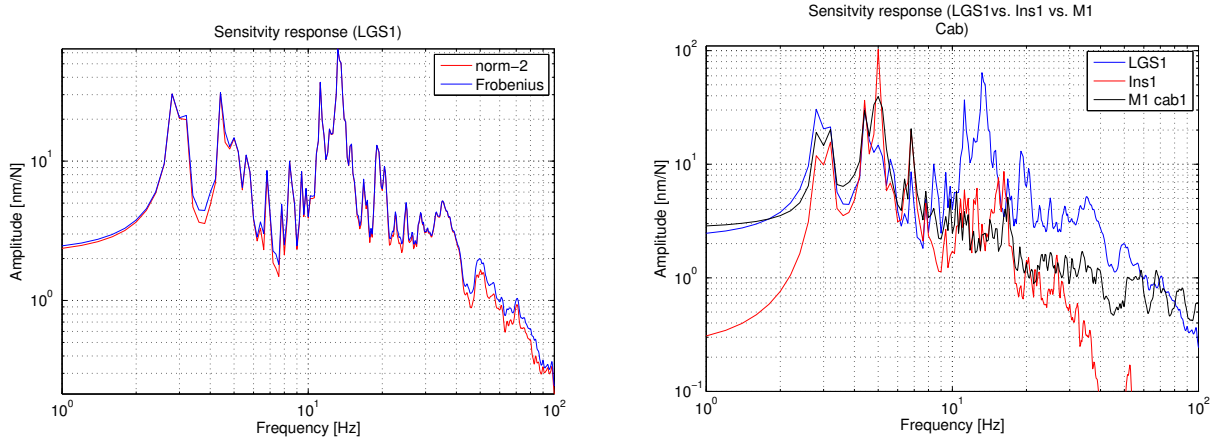


Figure 3. Transmission frequency response (nm/N) before AO-correction, vibration at LGS1 in (x, y, z) -directions; sensitivity defined by norm-2 and Frobenius norm (left), sensitivity response (Frobenius) from different vibration source locations, LGS1, Ins1, M1 cab1 (right)

Figure 3 shows the sensitivity response (represented by norm-2 and Frobenius norm of $\mathbf{H}_{\text{pttvib}}(j\omega)$) from the vibration sources assumed to be at LGS (near M1 cell). In the same figure the sensitivity responses for different location of vibration sources, i.e. Laser Guide Star #1 (LGS1), Instrument #1 on Nasmyth platform (Ins1), and a cabinet under segment subunits (M1 cab1) are compared to each other.

The sensitivity responses to the wavefront error are useful to identify the temporal frequency zones which influence most the error. However, no information on the spatial frequency modes of M1 can be directly extracted from them. For M1 system the segment phasing or the high spatial frequency behavior of the mirror are particularly important. The correction capability is not only limited by the temporal bandwidth of the AO system but also by the spatial behavior of the M1 mirror. For a given temporal frequency the higher spatial modes (large inter segment motions) are less effectively corrected by the AO system compared to the lower

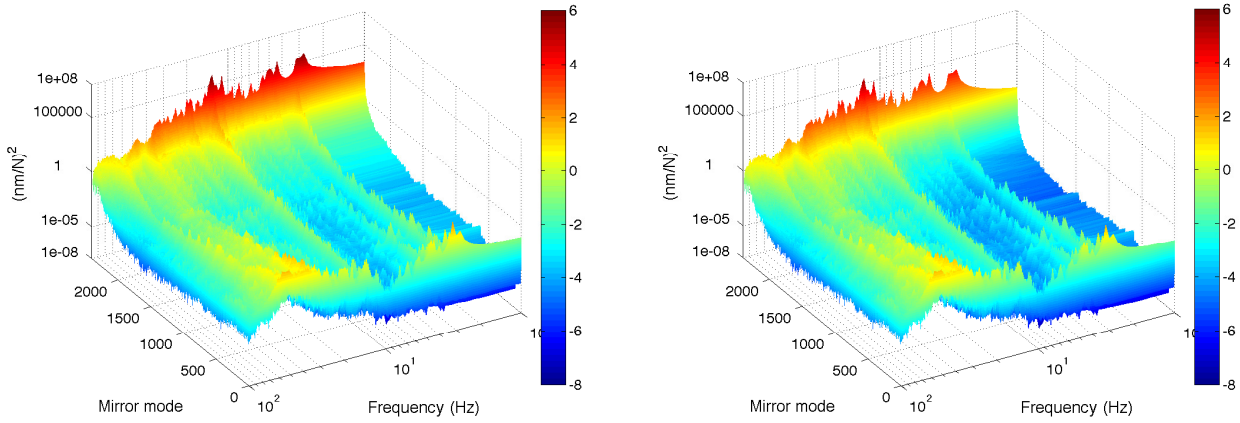


Figure 4. Vibration transmission sensitivity from LGS1 to M1 wavefront expressed in mirror modes for different temporal and spatial frequencies, before AO (left), after AO (right)

spatial modes (small inter segment motions and hence smoother M1). Therefore, it is important to understand and distinguish the sensitivity responses for different spatial modes of M1.

A potential and useful criterion is the response to different spatial modes (low to high) of M1 mirror. This can be obtained for instance by using the actuator-edge sensor interaction matrix ($IM = PACT2ES$) to project the PTT motions of the segments into a space representing the spatial modes of a segmented mirror. Figure 4 shows the sensitivity responses from a source located at LGS1 as a function of temporal and spatial frequencies before and after AO correction. *Mode#2394* represents the lowest spatial mode (M1 piston) and *Mode#1* the highest spatial mode respectively. It can be observed that the AO correction is more efficient for low spatial modes while the high spatial modes are not corrected by AO loops. Figure 5 shows the same response (before AO-correction) from a different view angle perspective.

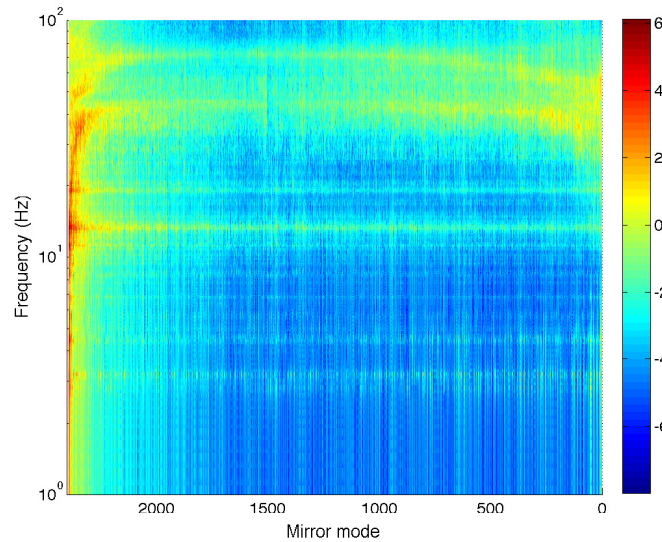


Figure 5. Vibration transmission sensitivity from LGS1 to M1 wavefront expressed in mirror modes $(nm/N)^2$ for different temporal and spatial frequencies, before AO

Vibration sources characteristics (amplitude and frequency contents) are quite uncertain and unknown at

this stage of the project. It would be impossible to characterize and understand all possible vibration sources in the lifetime of the telescope. Nevertheless, there are ongoing efforts to measure/characterize and model some 'outstanding' sources, such as fans, pumps, electrical and cooling systems. From the past experiences (measurements/literature) it is known that the vibrational forces are exhibiting a combination of both wide band (white noise) and narrow band (harmonics) behavior. However, the amplitude and the exact frequencies are less understood.

At this stage of the project it is important i) to understand the mechanism of the transmission of vibration at different locations of the telescope and their impact on the wavefront (space-time behavior), and ii) to identify and derive the maximum allowable forces/motions of sources leading to an acceptable observatory performance/budget. The second point is discussed in the next section. To develop and satisfy the first objective, the motions of M1 segments due to the different vibration source locations in the telescope and various types of excitations are simulated (see Section 3 for the approach). White noise, harmonic signals, repetitive impulses and measured data are among the various types of excitations injected into the system.

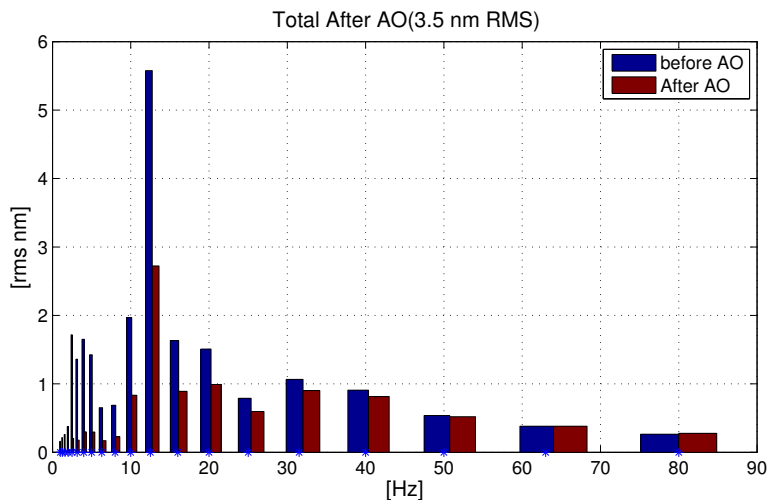


Figure 6. M1 WFE rms before and after AO correction due to vibrations forces at LGS1 with 1 [N] rms for different frequency bands

Figure 6 shows the wavefront error rms before and after AO correction for excitations (white noise in x , y and z direction) at the location of LGS1. The excitations are assumed to have a rms of 1 [N] (white noise with spectral density of $0.1 \text{ N}/\sqrt{\text{Hz}}$, [0-100] Hz). The contributions to the total wavefront error at different frequency bands are calculated and depicted in the same figure, where the temporal correcting limitation of the AO system (AO bandwidth: 30Hz) can also be observed.

Figure 7 shows a snapshot of the M1 mirror due to vibrations at the LGS1 location (at the top right of the M1). Left figure assumes white noise excitations in $(x, y$ and $z)$ direction with 1 [N] rms ($0.1 \text{ N}/\sqrt{\text{Hz}}$, [0-100] Hz) and right figure assumes a train of impulse with an amplitude of 1 [N] accruing every 2 seconds. The snapshot is taken shortly after the impulse is applied to the structure.

Figure 8 shows a snapshot of the M1 mirror due to vibrations at the Ins1 location. Left figure assumes white noise excitations in $(x, y$ and $z)$ direction with 1 [N] rms ($0.1 \text{ N}/\sqrt{\text{Hz}}$, [0-100] Hz) and right figure assumes a train of impulse with 1 [N] amplitude accruing every 2 seconds. The snapshot is made shortly after the impulse is applied to the structure.

5. REQUIREMENTS AND VIBRATION BUDGET

A wavefront error budget, which covers the allocation of vibration sources and contributors to the wavefront error after various corrections, e.g. field stabilization, adaptive optics (AO) is constructed. The budget items are

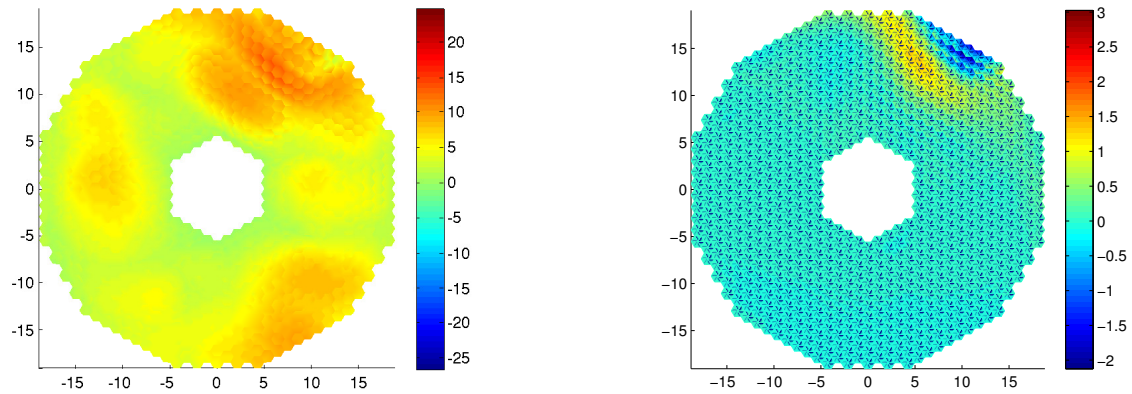


Figure 7. A snapshot of M1 segment motions due to vibrations at LGS1; (left) white noise force with 1[N] rms, (right) train of impulses with 1 [N] amplitude. Mechanical motions are in [nm] and x-y axes representing M1 dimensions are in [m]

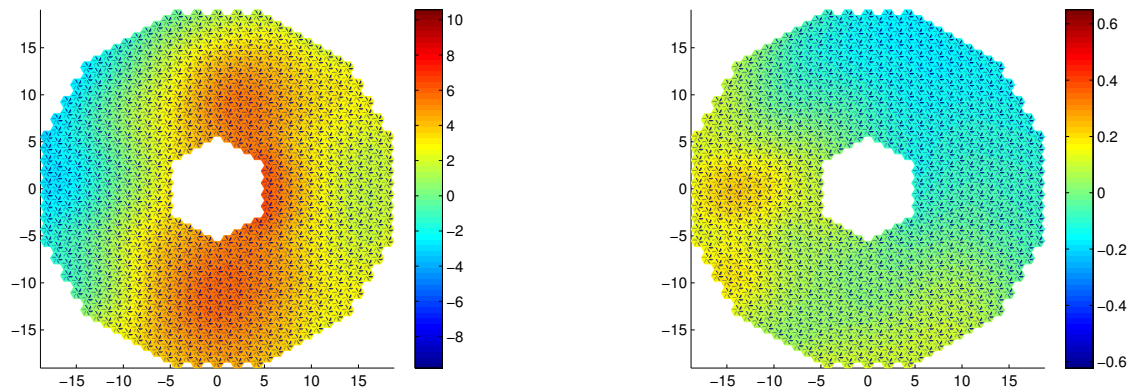


Figure 8. A snapshot of M1 segment motions due to vibrations at Ins1; (left) white noise force with 1[N] rms, (right) train of impulses with 1 [N] amplitude. Mechanical motions are in [nm] and x-y axes representing M1 dimensions are in [m]

broken down into the main products of the telescope such as Dome/Main structure, M1 to M5 units, Instruments etc. Each contributor includes different sources of vibration. For instance, cooling lines and cable wraps are the sources of vibration belonging to the Main Structure, while pumps, chillers and air handlers belonging to dome and facility buildings.

The budgeting is assumed to be an iterative approach: i.e. the allocations are at the level of each product breakdown. As the design advances and in future iterations a more detailed breakdown will be made. Also, a top down ad hoc allocation is adopted where performance/allocation is defined by the root mean square (rms) of the temporal wavefront error signal expressed in nanometer [nm]. A total wavefront of 50 [nm] rms (both temporal and statistical realization) is assumed for all vibrational sources and contributors.

As mentioned earlier, the key element for understanding and budgeting the vibrations is the sensitivity analysis. It provides an estimate of the wavefront error as a function of vibrational sources, location, amplitude and frequencies. Since the sensitivity is not uniform over all temporal frequency ranges, it follows logically that the requirements have to be partitioned and defined for different frequency zones.

It is clear that the exact frequency and shape of the mechanical modes in the model are not necessarily identical to those of the final design. Nevertheless, as it can be seen later the average shape of the response is

mainly defined by general physical behavior of the telescope, which is expected not to vary dramatically during the different design phases of the telescope and even after its realization: for instance the telescope inertia, overall stiffness, the estimated main axes and wavefront control bandwidths, and optical sensitivity are expected to change little during the final phases of telescope design. In addition, lower bounds for some key mechanical modes of the telescope structure or the units have been specified. This implies that the amplification of vibrations due to some sensitive local modes is not expected below certain known frequencies.

In addition to the modeling uncertainties, there are multiple vibration sources/transmission functions which contribute to the wavefront error. It would be cumbersome and none trivial/realistic trying to guess and derive the requirements for each possible source and direction individually using the models as they are. Therefore, to cope both with modeling uncertainties and multiple sources and directions, some conservatism is introduced by a special treatment of the sensitivity or transmission functions and grouping vibration sources with different directions into one entry using MIMO (multi-input multi-output) mathematical tools.⁷

The first level of conservatism is introduced by looking to the worst-case direction for all possible directions the vibration input source could generate an error. This is mathematically defined by norm-2 or the largest singular value of the transmission frequency responses used to define the WFE rms of M1 and introduced as the wavefront sensitivity responses. The second level of conservatism is then introduced by replacing the response in a certain frequency zone by its largest amplitude in that frequency band. This is mathematically equivalent to using the norm-infinity of the transmission frequency response on that specific band, i.e. $\|\mathbf{H}_{\text{pttopvib}}(j\omega)S(j\omega)\|_{\infty}$ $\forall \omega \in [\omega_i, \omega_j]$, where $S(j\omega)$ is the wavefront control rejection frequency response, e.g. AO loop.

Using the norm inequalities, it can be shown that the total rms wavefront error of M1, $\|WFE_{M1}\|_2$ (norm-2) is always smaller than the multiplication of the inputs norm-2 (rms of the vibration source forces/motions $\|U_{vib}\|_2$) and the infinity norm of the frequency response for each frequency interval, that is:

$$\|WFE_{M1}\|_2 \leq \|\mathbf{H}_{\text{pttopvib}}(j\omega)S(j\omega)\|_{\infty} \|U_{vib}\|_2, \quad \forall \omega \in [\omega_i, \omega_j] \quad (5)$$

The wavefront error is guaranteed to be smaller than the estimated value as long as the vibration source amplitudes remain smaller than the specified values. One advantage of such an approach is that once the maximum transmission in a frequency interval is obtained the wavefront estimation and requirement derivation/verification reduces to multiplication of two values and this can be done fast and iteratively. The approach is demonstrated through an example in the next section

Example: vibration requirement (allowable forces) and budget (estimated WFE)

For a given source, the vibration requirements are defined as allowable rms forces (root sum square of three directional forces) that lead to a wavefront error satisfying the budgeted value for that specific source item. Precisely, it is defined as the maximum allowable rms of forces for different frequency bands (here 1/3-octave bands).

As explained earlier the approach adds some conservatism. From one side this is sought and required for contingency and safety margin. But from the other side it could lead to restrictive requirements that are either unrealizable or unnecessary. To verify the degree of conservatism, the wavefront error values were compared for different sensitivity responses once assuming the worst case approach and once using the responses directly. Same input rms values were assumed for both cases. Depending on the source and location of the vibration, it was observed that a conservatism factor between 2 to 6 is involved in the estimations. Figure 9 shows the comparison between the M1 wavefront error from the worst case and direct calculation assuming the vibration source at location of LGS1. In this case at the worst case estimation is about 4 times larger than the direct response calculation.

To balance the excessive degree of conservatism, it was decided to include a factor 2.5 in all estimations. For instance assuming the allowable rms forces at their maximum level over all frequencies and using the worst case calculation, a wavefront of 10 [nm] rms corresponds to a budgeted value of $10/2.5 = 4$ [nm] rms.

Figure 10 shows the force requirement at LGS1 (root sum square RSS of the forces rms, top left), the worst direction and amplitude transmission responses (after AO correction, bottom left) and finally their multiplication band per band (right). The results are the upper bounds on the estimated wavefront for each frequency band.

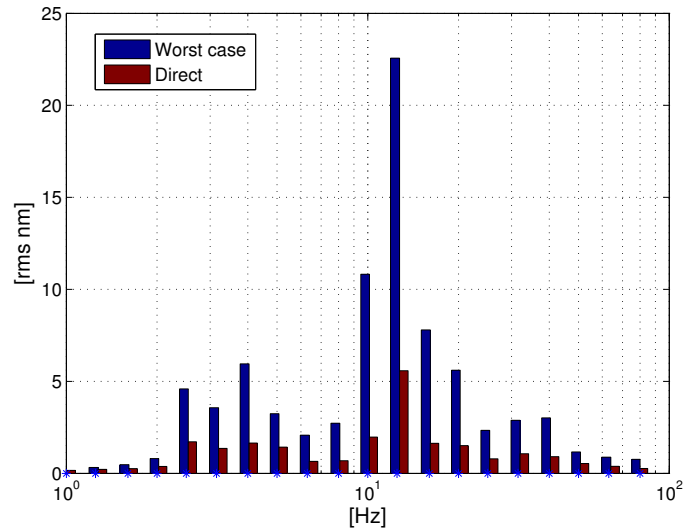


Figure 9. M1 WFE estimation: worst case calculation vs. direct calculation for a given input excitation at LGS1

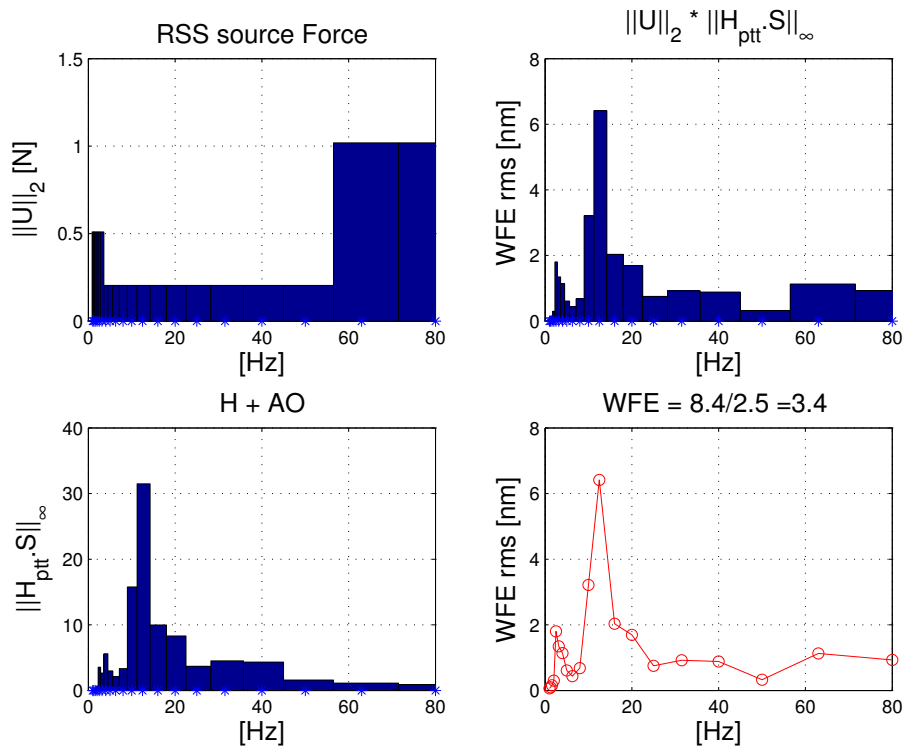


Figure 10. (top left): specified maximum rms of interface forces (RSS of all input forces) in [N]; bottom left: norm-infinity (maximum amplitude of worst direction) of the transmission frequency responses from LGS #3 to wavefront error; right (up and bottom): estimated worst case wavefront from the specification and the budgeted WFE value

The total M1 wavefront error (worst case) for this source of vibration is 8.4 [nm], which corresponds to a budget value of $8.4/2.5 = 3.4$ [nm] rms.

6. CONCLUSIONS

A model-based vibration analysis and budgeting for the M1 segmented mirror is presented. The modeling and budgeting of vibrations at early stages of the observatory design complements the common best effort practice of avoiding/isolating the vibrational sources. A sensitivity analysis is at heart of the effort to understand the mechanism of transmission of vibration forces to M1 mirror and its effect on the wavefront error. The combined finite element, control and optical models of the telescope and M1 segments are used to perform such a sensitivity analysis. Different parametric options and cases, e.g. position actuator types and control, were analyzed and compared. The analysis identifies the most sensitive locations of vibration sources and frequency zones which affect most the performance of M1 mirror and consequently the telescope overall performance. Since the phasing and relative motion of segments are crucial in the final performance of the telescope, a special attention was made to distinguish the contributions of vibration in different M1 spatial and temporal frequencies. In addition, temporal responses of the mirror for various types and kinds of excitations were derived and visualized. The visualization of M1 shape in time, was a big asset to understand and cross-check the validity of the results expressed in the frequency domain.

The vibration requirements, expressed in terms of rms force/motion in different frequency intervals, are basically derived from the sensitivity responses. To reduce the risks related to the uncertainties and inaccuracies of models and complex/multi directional propagation of vibrational forces in telescope, a conservative approach was developed. The approach uses the tools and technics common in MIMO systems to identify the largest possible amplification and direction of vibration for a given frequency interval. The degree of conservatism was studied and a safety factor was identified and used to relate the worst case results to the final budgeted vibration values.

REFERENCES

- [1] B. Sedghi, M. Müller, H. Bonnet, M. Esselborn, M. L. Louarn, R. Clare, and F. Koch, “E-ELT modeling and simulation toolkits: philosophy and progress status,” in *Symposium on Integrated Modeling of Complex Optomechanical Systems*, A. Enmark and T. Andersen, eds., *Proc. SPIE*, 2011.
- [2] B. Sedghi, M. Müller, and G. Jakob, “E-ELT vibration modeling, simulation, and budgeting,” in *IMCOS15 Integrated Modeling of Complex Optomechanical Systems II (IMC15)*, *Proc. SPIE*, 2015.
- [3] D. G. MacMartin and H. Thompson, “Equipment vibration budget for the TMT,” in *Ground-based and Airborne Telescopes V*, L. M. Stepp, R. Gilmozzi, and H. J. Hall, eds., *Proc. SPIE* **9145**, 2014.
- [4] H. Thompson, D. G. MacMartin, P. W. G. Byrnes, D. Tomonod, and H. Teradad, “Measuring transmission and forces from observatory equipment vibration,” in *Ground-based and Airborne Telescopes V*, Ground-based and A. T. V, eds., *Proc. SPIE*, 2014.
- [5] B. Sedghi, M. Dimmler, M. Müller, and N. Kornweibel, “Improving E-ELT M1 prototype hard position actuators with active damping,” in *Ground-based and Airborne Telescopes IV*, *Proc. SPIE*, 2016.
- [6] M. Müller and F. Koch, “System analysis tools for an ELT at ESO,” in *Modeling, Systems Engineering, and Project Management for Astronomy II*, M. Cullum and G. Angeli, eds., *Proc. SPIE* **6271**, 2006.
- [7] S. Skogestad and I. Postlethwaite, *Multivariable Feedback Control, Analysis and Design, Second Edition*, John Wiley and Sons Ltd, 2005.